

Study of quantum confinement effects on hole mobility in silicon and germanium double gate metal-oxide-semiconductor field-effect transistors

Chun-Jung Tang, Tahui Wang, and Chih-Sheng Chang

Citation: *Applied Physics Letters* **95**, 142103 (2009); doi: 10.1063/1.3244205

View online: <http://dx.doi.org/10.1063/1.3244205>

View Table of Contents: <http://scitation.aip.org/content/aip/journal/apl/95/14?ver=pdfcov>

Published by the *AIP Publishing*

Articles you may be interested in

Dramatic enhancement of low electric-field hole mobility in metal source/drain Ge p-channel metal-oxide-semiconductor field-effect transistors by introduction of Al and Hf into SiO₂/GeO₂ gate stack

Appl. Phys. Lett. **103**, 122106 (2013); 10.1063/1.4821546

Channel direction, effective field, and temperature dependencies of hole mobility in (110)-oriented Ge-on-insulator p-channel metal-oxide-semiconductor field-effect transistors fabricated by Ge condensation technique

J. Appl. Phys. **109**, 033709 (2011); 10.1063/1.3537919

Physics of strain effects in semiconductors and metal-oxide-semiconductor field-effect transistors

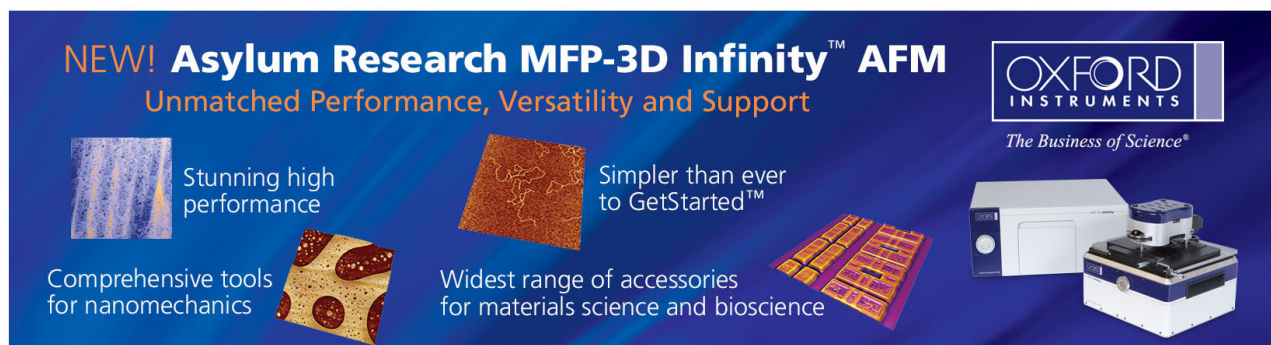
J. Appl. Phys. **101**, 104503 (2007); 10.1063/1.2730561

Valence band structure of ultrathin silicon and germanium channels in metal-oxide-semiconductor field-effect transistors

J. Appl. Phys. **98**, 024504 (2005); 10.1063/1.1948528

Hole confinement and mobility in heterostructure Si/Ge/Si p-channel metal-oxide-semiconductor field effect transistors

J. Appl. Phys. **81**, 8079 (1997); 10.1063/1.365415



NEW! Asylum Research MFP-3D Infinity™ AFM
Unmatched Performance, Versatility and Support

OXFORD INSTRUMENTS
The Business of Science®

Stunning high performance
Simpler than ever to GetStarted™

Comprehensive tools for nanomechanics
Widest range of accessories for materials science and bioscience

Study of quantum confinement effects on hole mobility in silicon and germanium double gate metal-oxide-semiconductor field-effect transistors

Chun-Jung Tang,¹ Tahui Wang,^{1,a)} and Chih-Sheng Chang²

¹Department of Electronics Engineering, National Chiao-Tung University, Hsinchu 30050, Taiwan

²Taiwan Semiconductor Manufacturing Company, Hsinchu 30077, Taiwan

(Received 22 July 2009; accepted 15 September 2009; published online 5 October 2009)

Quantum confinement effects on hole mobility in silicon and germanium double gate *p*-channel metal-oxide-semiconductor field-effect transistors (MOSFETs) are studied by using a Monte Carlo method. Uniaxial stress and channel/substrate orientation effects are considered. Our result shows that the hole mobility in a (100)/[110] silicon well decreases with a decreasing well thickness, which is in agreement with the experimental result. The hole mobility in a germanium channel MOSFET, however, exhibits a peak in a sub-20 nm well because of the interplay between intrasubband and intersubband scatterings. © 2009 American Institute of Physics. [doi:10.1063/1.3244205]

Double-gate (DG) metal-oxide-semiconductor field-effect transistors (MOSFETs) and fin field-effect transistor have been considered as promising alternatives to bulk MOSFETs in 22 nm technology node and beyond^{1–3} due to their immunity to short channel effects. Recently, advanced channel materials with higher carrier mobility than bulk Si, such as Ge (Ref. 4) and III-V materials,⁵ have attracted much attention. Experimental works have shown the possibility that the inversion carrier mobility can be further improved in quantum structure MOSFETs by a subband modulation.^{6,7} However, there has been little work on Ge-channel DG-pMOSFETs addressing valence subband and substrate/channel orientation effects on hole mobility.

In this paper, we analyze quantum confinement effects on hole mobility as a function of a body thickness in Si- and Ge-channel DG-pMOSFETs. The low-field hole mobility is calculated by a Monte Carlo method.⁸ The impact of substrate orientation on hole mobility is also evaluated. Furthermore, the effect of uniaxial compressive stress is discussed.

Instead of the effective-mass approximation, the valence subband structures for two-dimensional holes in Si- and Ge-channel DG-pMOSFETs are calculated self-consistently from the coupled Poisson and Schrödinger equations with a six-band Luttinger–Kohn Hamiltonian including spin-orbit coupling.⁹ The Bir–Pikus deformation potentials¹⁰ are also included to take into account the stress effect. In addition, an appropriate rotation matrix is employed when dealing with substrate orientations other than the (100) direction.^{11,12} Material parameters, including Luttinger parameters, deformation potentials, and elastic constants used in the simulation, are given in Refs. 13–15. Relevant scattering mechanisms, including acoustic phonon scattering, optical phonon scattering, and surface roughness scattering, are considered in the Monte Carlo simulation.^{16–19} The scattering parameters of Si and Ge are calibrated from a conventional Si MOSFET and from a SiGe-on-insulator device, respectively.¹⁸

Figure 1 compares the hole mobility as a function of a body thickness in (100)/[110] Si- and Ge-channel DG-pMOSFETs, where () and [] are the notations of substrate

orientation and channel direction, respectively. The choice of the [110] channel in Si is because it has a larger stress effect. The inversion hole density, p_{inv} , is set to be $4 \times 10^{12} \text{ cm}^{-2}$. The simulated hole mobility in a Si-channel decreases monotonically with a body thickness, which is consistent with the experimental data.⁶ Unlike a Si channel, the hole mobility in a Ge channel shows a turn-around characteristic with a body thickness. When a body thickness reduces, the hole mobility increases gradually to a maximum around $T_{Ge}=16 \text{ nm}$, and then decreases drastically. In the window of inversion hole density and body thickness considered in this work, where the transverse effective electric field is about 0.12 MV/cm in a Ge channel, the surface roughness scattering has a minor effect on the hole mobility in a Ge channel. The same conclusion can be found in Ref. 20. Therefore, surface roughness scattering should not affect the existence of a mobility peak in a Ge channel. Moreover, the calculated hole mobility at $T_{Ge}=28 \text{ nm}$ is about $617 \text{ cm}^2/\text{V s}$, which deviates from the bulk value of Ge. This is due to larger phonon deformation potentials in a MOSFET than in a bulk material, resulting from stress at gate dielectric and semiconductor interface.²¹

The turn-around behavior of the mobility in a Ge-channel can be explained in the two following aspects: overlap integral and energy separation between subbands. As a

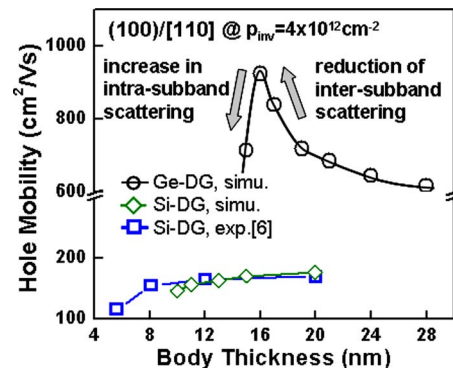


FIG. 1. (Color online) Simulated hole mobility as a function of a body thickness in (100)/[110] Si- and Ge-channel DG-pMOSFETs. The experimental result for Si channels is plotted for comparison.

^{a)}Electronic mail: twang@cc.nctu.edu.tw.

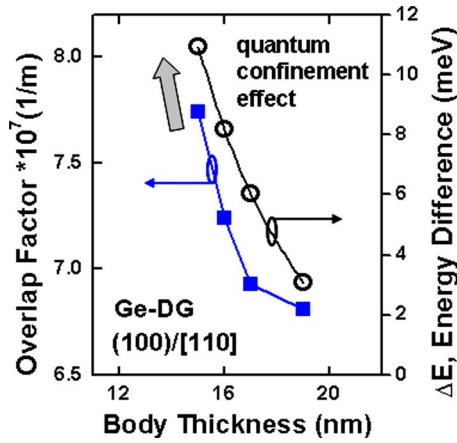


FIG. 2. (Color online) The body thickness dependence of an overlap factor and an energy difference between the lowest two subbands in (100)/[110] Ge-channel DG-pMOSFETs.

body thickness decreases, the energy difference, ΔE , between the first subband (heavy hole band) and the second subband (heavy hole band) increases owing to quantum confinement effects, as shown in Fig. 2. Because of less chance to be scattered to the second subband, inversion holes have a larger mobility owing to a smaller intersubband scattering rate. On the other side, the intrasubband scattering rate increases due to an increase of an overlap integral. The confinement effect on the overlap integral can be understood from the illustration in Fig. 3. When a smaller body thickness is considered, the wave function has a wider distribution in momentum space due to the uncertainty principle. For a fixed phonon momentum in the quantized direction q_z , only the shaded region in Fig. 3 contributes to the overlap integral. A broader distribution in momentum space results in a larger overlap factor (Fig. 2) and thus a larger intrasubband scattering rate. The interplay between intersubband and intrasubband scatterings opens a window of a body thickness where the scattering rates can be minimized, giving rise to a peak in hole mobility, as shown in Fig. 1. Unlike a Ge channel, the lowest two subbands in a (100)/[110] Si channel are heavy-hole and light-hole bands, respectively, due to the high degree of degeneracy of heavy and light holes in Si.⁷ For a decreasing well thickness, the larger energy separation reduces hole population in the light-hole subband and leads to a decrease of hole mobility.

Moreover, the substrate orientation effect in Ge channels is evaluated in Fig. 4. The same scattering parameters of

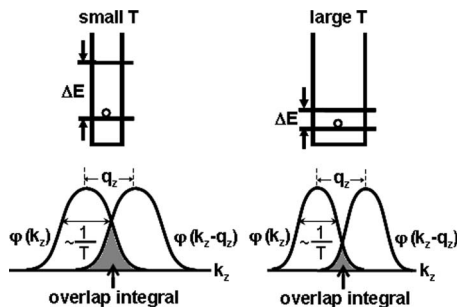


FIG. 3. Illustration of the body thickness dependence of valence subband energy and overlap factor. The shaded region corresponds to an overlap integral. A narrower quantum well has a larger energy separation between subbands and a larger overlap factor.

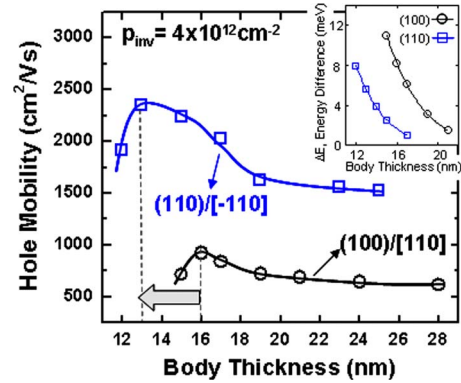


FIG. 4. (Color online) Comparisons of the hole mobility and subband energy difference in (100)/[110] and (110)/[110] Ge-channels.

surface roughness scattering for (100) and (110) substrates are assumed. Three points are worth noting. First, quantum confinement induced mobility enhancement is again observed in (110) substrate. Second, the (110) substrate shows an anisotropy of energy dispersion, such that the (110)/[110] channel direction exhibits a highest mobility, and then the (110)/[001] (result not shown in Fig. 4). The higher mobility in (110)/[110] than in (100)/[110] is attributed to a lower conductivity effective mass. Third, the peak mobility in (110)/[110] occurs at a smaller body thickness. This reason is that a smaller energy difference between the lowest two subbands is obtained in Ge (110) substrate.

Finally, the effect of 0.3 GPa uniaxial compressive stress on normalized hole mobility is shown in Fig. 5. Note that the channel direction is also the uniaxial stress direction. Generally, the uniaxial compressive stress removes the heavy hole and light hole degeneracy and alters the warping of the valence bands. Thus, the effective mass becomes anisotropic with applied stress. The constant energy contours of the first subband for (100) and (110) substrates are depicted in the figure. In Fig. 5, at a large body thickness, the stress induced hole mobility enhancement in (100)/[110] and (110)/[110] channel directions is comparable due to the same bulk piezoresistance coefficients.²² For a smaller body thickness, the quantum confinement effect plays a role and the energy difference from the uniaxial compressive stress and surface

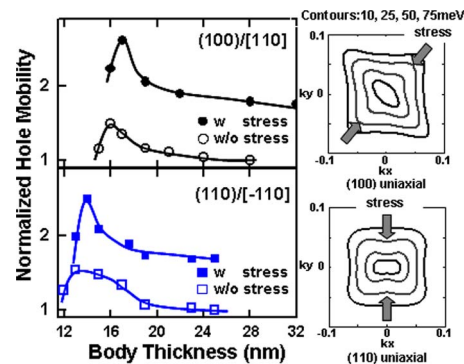


FIG. 5. (Color online) Ge hole mobility as a function of a body thickness in (100)/[110] and (110)/[110] channel directions with and without an uniaxial compressive stress of 0.3 GPa. The mobility is normalized to the one without stress effect. The constant energy contours in (100) and (110) substrates are also plotted.

field is additive, which is responsible for the slight shift of the peak mobility.

In conclusion, the effects of channel/substrate orientation and uniaxial compressive stress on hole mobility versus body thickness in Ge-channel DG-pMOSFETs are investigated. The peak mobility in both (100)/[110] and (110)/ $[\bar{1}10]$ channel directions can be achieved at a certain body thickness due to the interplay between intersubband and intrasubband scatterings. Furthermore, the hole mobility can be further improved when the uniaxial compressive stress is applied to (100)/[110] or (110)/ $[\bar{1}10]$ channel direction.

The authors (C.J.T., T.W., and C.S.C.) would like to acknowledge financial support from National Science Council, Taiwan, under Contract No. NSC-96-2628-E-009-165-MY3 and from Taiwan Semiconductor Manufacturing Co.

- ¹F. Balestra, S. Cristoloveanu, M. Benachir, J. Brini, and T. Elewa, *IEEE Electron Device Lett.* **8**, 410 (1987).
²H. Kawasaki, M. Khater, M. Guillorn, N. Fuller, J. Chang, S. Kanakasa-bapathy, L. Chang, R. Muralidhar, K. Babich, Q. Yang, J. Ott, D. Klaus, E. Kratschmer, E. Sikorski, R. Miller, R. Viswanathan, Y. Zhang, J. Silverman, Q. Ouyang, A. Yagishita, M. Takayanagi, W. Haensch, and K. Ishimaru, *Tech. Dig. - Int. Electron Devices Meet.* **2008**, 237.
³T. Mérelle, G. Curatola, A. Nackaerts, N. Collaert, M. J. H. van Dal, G. Doornbos, T. S. Doorn, P. Christie, G. Vellianitis, B. Duriez, R. Duffy, B. J. Pawlak, F. C. Voogt, R. Rooyackers, L. Witters, M. Jurczak, and R. J. P. Lander, *Tech. Dig. - Int. Electron Devices Meet.* **2008**, 241.
⁴R. Xie, T. H. Phung, W. He, Z. Sun, M. Yu, Z. Cheng, and C. Zhu, *Tech. Dig. - Int. Electron Devices Meet.* **2008**, 393.
⁵N. Goel, D. Heh, S. Koveshnikov, I. Ok, S. Oktyabrsky, V. Tokranov, R.

- Kambhampati, M. Yakimov, Y. Sun, P. Pianetta, C. K. Gaspe, M. B. Santos, J. Lee, S. Datta, P. Majhi, and W. Tsai, *Tech. Dig. - Int. Electron Devices Meet.* **2008**, 363.
⁶S. Kobayashi, M. Saitoh, and K. Uchida, *Tech. Dig. - Int. Electron Devices Meet.* **2007**, 707.
⁷G. Tsutsui, M. Saitoh, and T. Hiramoto, *Dig. Tech. Pap. - Symp. VLSI Technol.* **2005**, 76.
⁸C. Jacoboni and L. Reggiani, *Rev. Mod. Phys.* **55**, 645 (1983).
⁹J. M. Luttinger and W. Kohn, *Phys. Rev.* **97**, 869 (1955).
¹⁰G. L. Bir and G. E. Pikus, *Symmetry and Strain-Induced Effects in Semiconductors* (Wiley, New York, 1974).
¹¹A. T. Pham, C. Jungemann, and B. Meinerzhagen, *Solid-State Electron.* **52**, 1437 (2008).
¹²S. Rodríguez, J. A. López-Villanueva, I. Melchor, and J. E. Carceller, *J. Appl. Phys.* **86**, 438 (1999).
¹³T. Low, M. F. Li, Y. C. Yeo, W. J. Fan, S. T. Ng, and D. L. Kwong, *J. Appl. Phys.* **98**, 024504 (2005).
¹⁴J. D. Wiley, *Solid State Commun.* **8**, 1865 (1970).
¹⁵M. V. Fischetti and S. E. Laux, *J. Appl. Phys.* **80**, 2234 (1996).
¹⁶M. V. Fischetti, Z. Ren, P. M. Solomon, M. Yang, and K. Rim, *J. Appl. Phys.* **94**, 1079 (2003).
¹⁷M. De Michielis, D. Esseni, Y. L. Tsang, P. Palestri, L. Selmi, A. G. O'Neill, and S. Chattopadhyay, *IEEE Trans. Electron Devices* **54**, 2164 (2007).
¹⁸A.-T. Pham, C. Jungemann, and B. Meinerzhagen, *IEEE Trans. Electron Devices* **54**, 2174 (2007).
¹⁹S. E. Thompson, G. Sun, Y. S. Choi, and T. Nishida, *IEEE Trans. Electron Devices* **53**, 1010 (2006).
²⁰L. Donetti, F. Gamiz, F. G. Ruiz, N. Rodriguez, and A. Godoy *Proceeding of the Meeting Abstracts of the Journal of the Electrochemical Society*, 2009 (unpublished), Vol. 901, p. 959.
²¹M. Lundstrom, *Fundamentals of Carrier Transport*, 2nd ed. (Cambridge University Press, Cambridge, 2000).
²²C. S. Smith, *Phys. Rev.* **94**, 42 (1954).